CO_2 permeation through fusion-bonded epoxy coating in humid environments

Hossein Zargarnezhad [a,*], Kashif Mairaj Deen [a], Dennis Wong [b], C.N. Catherine Lam [b], Edouard Asselin [a]

[a] *The University of British Columbia, Department of Materials Engineering, 309-6350 Stores Road, Vancouver, BC V6T 1Z4, Canada*

[b] *Shawcor Ltd., 25 Bethridge Road, Toronto, ON, M9W 1M7, Canada*

**Corresponding author: hossein.zargar@ubc.ca (H. Zargarnezhad)*

ABSTRACT

This study investigates the effect of water and CO_2 exposure on the performance of epoxy-based coatings under conditions commonly found in pipeline applications. The permeability of fusion bonded epoxy (FBE) decreases as CO_2 pressure increases and the presence of water facilitates gas transport through the coating. The latter is in conflict with theories of membrane selectivity and competitive transport in gas/vapor systems, in which water is the predominant permeant for its lower kinetic diameter and higher condensability. Our results show that this anomaly was due to the dynamic transformation of permeable channels in the coating structure. Microstructural characterization of FBE after exposure to CO_2/H_2O mixtures showed that carbonation of wollastonite filler particles results in a change in shape, volume, and chemical composition of these filler particles. The chemical reaction between wollastonite and CO_2 in the presence of water led to a degradation that caused changes in porosity, permeability, and filler volume. To verify these findings for the coating in the presence of adhesion forces, electrochemical impedance spectroscopy (EIS) was also used. The tests conducted showed that exposure to a CO_2/H_2O mixture causes filler particles within the coating to undergo carbonation, leading to the formation

of new microchannels within the epoxy network. Initially, the carbonation of fillers led to an increase in the pore resistance of the coating, which was attributed to the plugging of micropore channels on the coating surface. However, the subsequent decreasing trend of this parameter suggested that water infiltration into the coating had increased due to this degradation. The carbonation of wollastonite within the FBE coating leads to a volume change in the fillers, resulting in the creation of small voids or gaps in the epoxy matrix. This, in turn, facilitates the easier penetration of water and dissolved gas to the underlying substrate. Consequently, the accumulation of water inside coating increases the dielectric constant, resulting in a higher capacitance of the coating. It appears that high concentrations of CO_2 in wet conditions, even at low pressures, can have negative impacts on the barrier performance of the coating.

KEYWORDS

Fusion bonded epoxy, CO_2 permeation, Competitive permeation, Carbonation, Wet-state diffusion.

1. Introduction

The increasing demand for energy has driven oil and gas producers to extract fossil fuels in challenging environments, where the conditions can have a significant impact on the design of coating systems for metal infrastructure such as pipelines [1]. This is especially true in the presence of water and carbon dioxide, where CO_2-rich environments can greatly increase the rate of uniform corrosion and pit formation [2]–[4]. Protective coatings and linings for process equipment and transportation pipelines typically utilize epoxy-based materials, which are susceptible to microstructural degradation in humid conditions [5]. The transport and sorption behavior of both water vapor and CO_2 in glassy polymers can differ greatly from other gas species, and while there is a significant body of research on CO_2 transport in these materials [6], [7], there is a lack of understanding of the synergistic effects of CO_2 and water vapor on epoxy coatings.

CO_2 is widely studied as a gas penetrant in glassy polymeric membranes, as it exhibits unique behavior in different polymers [8]. Unlike water vapor, CO_2 dissolution in glassy polymers typically follows the standard dual-mode sorption model, i.e., Henry's type sorption and Langmuir adsorption at microvoids. Additionally, individual transport of CO_2 does not cause plasticization in the polymeric network until the gas pressure reaches a relatively high critical value in the system (e.g., above 10 bars) [9]–[11]. In a study by Scholes et al. [6], the competitive sorption and transport of CO_2 and water vapor in high-free-volume glassy polymers was investigated. They found that water sorption leads to plasticization of a glassy polymeric membrane and results in competitive sorption with gaseous species such as CO_2 and N_2. Plasticization increases the diffusivity of permeants, but competitive sorption reduces diffusivity through clustering or blocking phenomena. The interplay between water vapor and CO_2 at the threshold of coating plasticization (i.e., *ca.* 65°C in most epoxy systems) is not well understood, and further measurements of gas permeation may provide insight into the extent of plasticization or competitive effects in humid environments. Also, examining how CO_2 exposure in wet environments affects the microstructure of coatings could lead to more accurate corrosion performance assessments in service conditions based on empirical mass transport data.

The glass transition temperature (T_g) of fusion bonded epoxy (FBE) is approximately 110°C and may vary depending on the formulation or ageing conditions [5]. Unlike glassy membranes, epoxy-based coatings do not exhibit pronounced selectivity in filtering one permeant over the other based on molecular size or polarity [12], [13]. However, the mechanisms of permeant dissolution and transport are similar, and the mass transport mechanism in coating structures follows the same principles as that of membrane separation. Modeling of steady-state permeability based on the solution-diffusion model requires sorption data of individual permeants, which are currently lacking in the literature. Therefore, in this study we directly examine the CO_2 permeation in the presence of water and discuss their combined effects on the degradation of the barrier epoxy structure.

The underlying mechanism of corrosion in coated metal infrastructure, such as pipelines, is complex and multi-faceted, involving a range of chemical, electrochemical, and transport phenomena [14]. As the barrier coating begins to degrade, the kinetics of each step can change. In environments saturated with CO_2 and water, the formation of carbonic acid and dissociation reactions can accelerate CO_2-induced corrosion:

$$CO_2(g) \leftrightarrow CO_2(aq) \quad (1)$$

$$CO_2(aq) + H_2O \leftrightarrow H_2CO_3 \quad (2)$$

$$H_2CO_3 \leftrightarrow H^+ + HCO_3^- \quad (3)$$

$$HCO_3^- \leftrightarrow H^+ + CO_3^{2-} \quad (4)$$

CO_2 dissolves in water forming carbonic acid, which is a weak acid that only partially dissociates [15]. In aqueous solutions with a *pH* above 6, carbon steel corrodes to form iron carbonate, among other oxides, due to the reduction of H_2CO_3, represented by reaction (3) [16], [17]:

$$Fe + 2e^- \rightarrow Fe^{2+} \quad (5)$$

$$Fe^{2+} + CO_3^{2-} \rightarrow FeCO_3 \quad (6)$$

For mildly acidic and alkaline environments (*pH* > 6), Fe_3O_4, $Fe(OH)_2$, and $FeCO_3$ can coexist. However, the most thermodynamically stable species of the three is $FeCO_3$ (i.e. it has the lowest Gibbs free energy [18], [19]). The corrosion rate of CO_2 is directly affected by pH [18], and local pH variations can occur at the surface of under-coating pipes [20]. This suggests that gas ingress through the coating may serve as a key indicator of these processes. Since the protection performance of a coating system can also be affected by factors such as adhesion and internal stresses, it is important to study both free standing coating films and coatings applied to substrates to gain a thorough understanding of a coating's performance [21], [22].

In this study, we focused on investigating the permeability of CO_2 through FBE, both individually and in combination with liquid water. We place particular emphasis on FBE, as it is the primary

protective component in epoxy-based systems. Multilayering approaches, such as the high-performance powder coating system, are effective in extending the lifetime of the FBE component because they reduce water transport [16]. At 65°C, FBE undergoes a plasticization process in humid environments, which can alter its barrier performance due to the formation of microcavities and the resulting segregation effects within the coating. Here, we examined the microstructural changes in the coatings caused by exposure to water and CO_2, and identified the synergistic effects of these permeants on the barrier coating. Ultimately, we studied the under-coating corrosion of the steel substrate by directly exposing FBE-coated steel panels to a CO_2 atmosphere in the presence of liquid water to characterize their electrochemical response.

2. Experimental

2.1. Membrane and coated panel preparation

We examined the properties of free-standing FBE coating films and FBE-coated steel panels with no macroscopic defects. The FBE coating is applied as a dry powder to a preheated substrate at a temperature of up to 245°C by the manufacturer. The FBE resin is a type of polymer that is composed of diglycidyl ether of bisphenol A (DGEBA) and dicyandiamide (DDA) as the main components [23], with mineral agents such as wollastonite ($CaSiO_3$), aluminum oxide and anatase titanium oxide added for improved performance [24], [25]. For free standing films, the manufacturer (Shawcor Ltd) applied the FBE powder on an easy release PTFE substrate. After removing the cured epoxy film from the PTFE substrate, disk-shaped specimens were cut from the film for use in experiments. FBE-coated panels were also prepared by applying the FBE powder on 1 cm thick steel plates. The cured epoxy film thickness was measured using standard procedures [26]. To remove any residual moisture for dry gas measurements, the samples were vacuum dried at 22°C for 3 days [27]. To minimize ageing effects, all samples were used within 5 days of vacuum drying [6].

2.2. CO_2/H_2O permeability measurements

We used an in-house designed and built constant pressure variable volume set-up, based on continuous-flow methods as illustrated in Fig. 1, to study the steady-state permeability of CO_2. A back-pressure controller was used to control the retentate gas flow, while a mass flow controller was used to control the nitrogen carrier gas flow. CO_2 (≥ 99.5%) and pure N_2 (≥ 99.995 %) were obtained from Linde Inc. (Canada). The upstream chamber was filled with a water/gas mixture and its temperature was regulated using an external coil. Prior to each test, both upstream and downstream chambers were connected to pure nitrogen gas. To maintain consistent test conditions, the flow rate of the gas in the downstream vessel was kept constant at 20 ml/min. After reaching a steady-state CO_2 concentration in the downstream volume (typically ~ 24 h), the upstream volume was partially filled with water and CO_2 gas was purged through a bubbler arrangement. The CO_2 and H_2O concentration in the permeate stream were monitored using a GasLab® Sensor Configuration/Data Logging Software (CM-0024, CO2Meter, USA) and a humidity sensor (SEK-SHT35, Sensirion, Switzerland) respectively, which were installed inside the gas flow chamber. To ensure good flow conditions without concentration polarization in the system, the feed flow rate was controlled at 1 L/min and the nitrogen sweep gas was at 20 mL/min on the permeate side. These rates were chosen for consistency with previous work in the literature on epoxy membranes [28]. Stainless steel wool was placed on the upstream side and a disk-shaped stainless steel wire mesh (thickness ~1.27 mm) on the downstream side of the membrane to promote mixing and avoid membrane deformation due to high-pressure exposure. Both sides of the coating membrane, with effective areas of 25 cm^2, were sealed with O-rings. Before each experiment, the permeation cell was pre-heated to the operating temperature and nitrogen was flowed through the top and bottom sides of the membrane for at least 24 hours to avoid potential vapor condensation during the experiment. Then, the upstream volume (~ 160 ml) was filled with water and the assembly was prepared for measurements. The total applied pressure was then adjusted according to the saturation pressure of water vapor (i.e., pressure gauge being the sum of atmospheric pressure, water vapor saturation pressure, and applied CO_2 partial pressure).

The diffusivity of permeant *i* can be estimated from the mass transport profile obtained from the permeant flow rate through the coating membrane, using both unsteady state and steady state measurements, as reported in reference [29]:

$$D_i = \frac{l^2}{7.199 t_{0.5}} \tag{7}$$

where l is thickness (m) of the membrane and $t_{0.5}$ denotes the time (s) at which the permeant flow rate reaches half of the flux at steady state conditions. Also, the permeation rate was described through a solution of Fick's second law for mass transfer [29], as follows:

$$P_i = \frac{J_\infty l}{\Delta p} \tag{8}$$

where P_i, J_∞, and Δp are the permeability coefficient (mol/m-s-Pa), the permeant flux at steady state (mol/m^2-s), and the partial pressure gradient of the permeant across the membrane (Pa), respectively. Our gas permeation apparatus was developed to measure permeability (P_{CO_2}) in wet-state conditions over a wide range of temperatures (25-80°C) and pressures (1-10 bar).

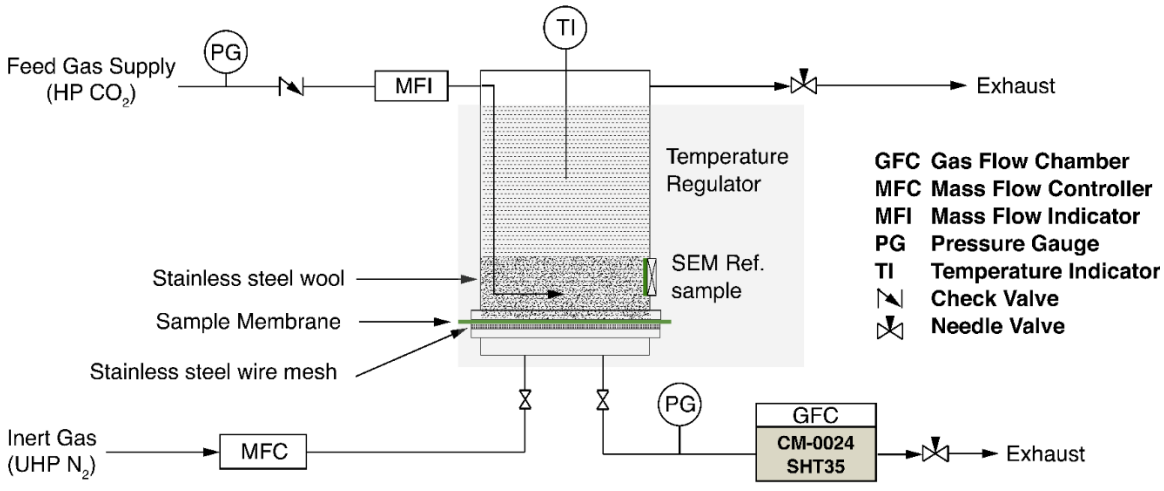

Fig. 1. CO_2 permeation apparatus for measurements on free-standing coating films. Spotted areas indicate liquid water in the shown volumes.

2.3. Microstructural characterization

To investigate the effects of wet gas mixture on the epoxy microstructure, free film samples were examined using a scanning electron microscope (SEM) equipped with an energy dispersive X-ray (EDX) detector (FEI Quanta 650, USA). These analyses were conducted at an accelerating voltage of 15 kV, a take-off angle of 0-20°, a working distance of 10-15 mm, and a sample chamber pressure of 10^{-4} Pa. For SEM analysis, a free film sample was mounted, polished and sputter-coated with a thin gold-palladium layer to provide conductivity. First, this mounted sample was used to study the composition and morphology of wollastonite filler particles in FBE. Then, it was placed in the upstream volume (as shown in Fig. 1) as a reference sample to study the interaction of water-dissolved CO_2 with the previously identified particles. For all SEM analysis, compressed clean air was used to remove debris from samples.

2.4. Applied coating performance: Electrochemical analysis

According to previous research conducted in our lab [16], the effects of transient sorption of water are most prominent during the initial 100 days of exposure, and since water has a relatively small kinetic diameter ($d_{CO_2}/d_{H_2O} = 1.245$), it is expected to act as the primary permeant in a binary CO_2/H_2O system [30]. Thus, we used coating panels that had been aged in 65°C deionized water for 120 days to simulate wet conditions. This was to eliminate effects of transient water sorption on the coating's response to a CO_2-rich medium during the specific timeframe being studied. The coated steel panels were analyzed using the test apparatus illustrated schematically in Fig. 2. A humid atmosphere was applied to the upstream chamber in Fig. 1 and directed onto the SEM reference sample via a bubbler arrangement at a controlled temperature. The exposure test was carried out at a CO_2 gas pressure of 800 kPa and 65°C. The coated steel panel was periodically removed from the chamber and analyzed via electrochemical impedance spectroscopy (EIS) at 65°C.

The non-destructive EIS measurements were performed via a custom-made electrochemical apparatus. The substrate of the coated steel panel served as the working electrode, a silver/silver chloride electrode as the reference electrode, and a platinum wire as the counter electrode. The coated panel was placed between a clean non-conductive benchtop and a rectangular testing cell (including a gasket). The exterior walls of the testing cell were tightly wrapped with copper tubing, which was used to maintain a temperature of 65°C by circulating water from a Cole-Parmer Polystat Heated Circulator (Antylia Scientific Co., USA). The active area for EIS measurement, after the tubing was clamped onto the coated panel, was 9.27 cm^2. A 3.5 wt% NaCl solution was used as the electrolyte. Measurements were taken using a Princeton Applied Research VersaSTAT 3F potentiostat, and data were captured with the VersaStudio software package. We conducted exposure tests for up to 300 h and performed two replicates to verify the results. After the open-circuit potential (OCP) of the coated steel reached a steady value (usually at –0.550 V vs. Ag/AgCl for 15 min at 65°C), the EIS measurement was conducted under a sinusoidal excitation potential of 10 mV RMS in the frequency range from 100 kHz to 0.1 Hz. To ensure the reproducibility of the results, EIS measurements were conducted at least three times under identical conditions. Data analysis was conducted using the *ZSimpWin* software and classical Equivalent Electrical Circuits (EEC).

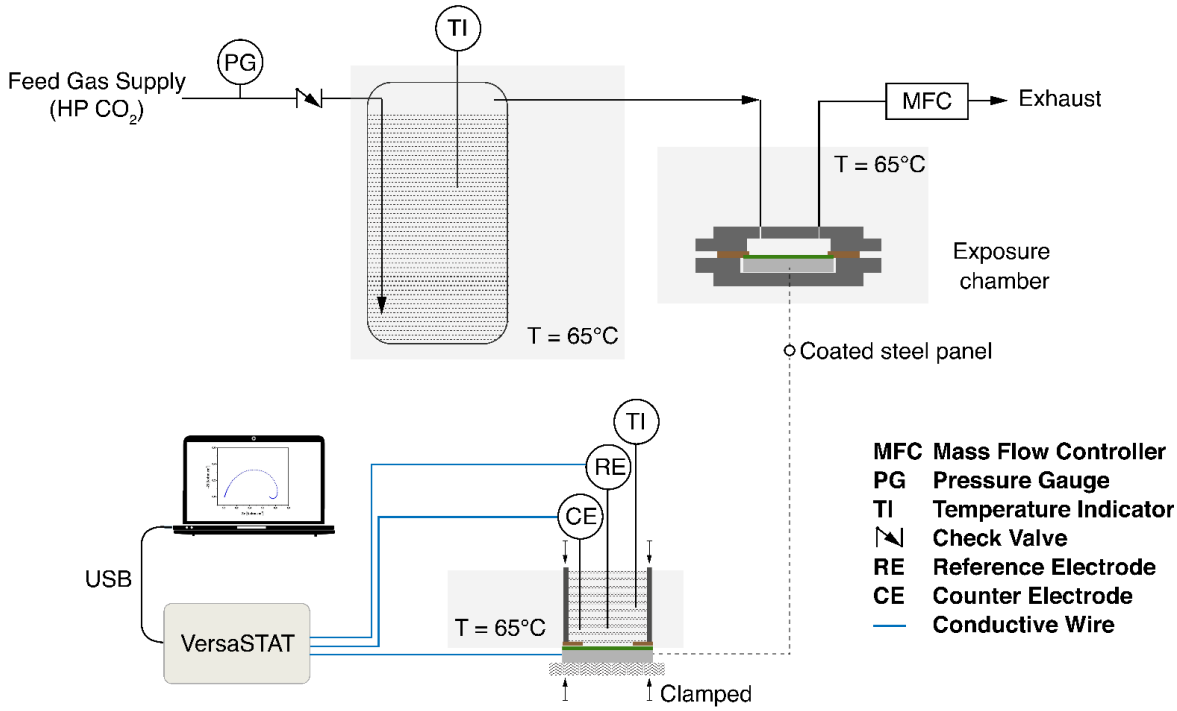

Fig. 2. Schematic illustration of performance tests on coated steel panels exposed to CO_2 at 100% relative humidity.

3. Results and discussion

3.1. Dry-state diffusion

The limited data available on the mass transport properties of CO_2 in epoxy materials prompted us to initially investigate CO_2 gas permeation in the absence of liquid water in the upstream volume. As shown in Fig. 3, we measured the CO_2 flux through FBE at various upstream pressures in a dry upstream volume at a temperature of 65°C. A similar procedure was followed for temperatures of 25, 40, 70, and 80°C as for 65°C. However, at ambient temperatures of 25 and 40°C, the flux values were too minor to be included in the results presented here. With Eq. (7) and (8), we were able to estimate the diffusivity and permeability parameters of CO_2 through the FBE. Table 1 presents the diffusivity coefficients at temperatures between 65, 70 and 80°C. These values

suggest that the mobility (or diffusivity) of CO_2 in FBE is low, two orders of magnitude less than that observed in high-density polyethylene [30]. This is in agreement with the reported diffusivity range for glassy polymers [8]. It is crucial to note that pipeline coatings are usually not impacted by high CO_2 pressure atmospheres. As such, the diffusivity of CO_2 in these coatings is independent of gas pressure within service conditions (i.e., up to 1 bar CO_2) and is quantified by the infinite dilution mobility coefficient (i.e. the diffusion coefficient of CO_2 in near zero upstream pressures of CO_2). Fig. 4 shows that the permeability of CO_2 decreases as the upstream pressure increases. This trend is consistent with data found in literature for commercial bisphenol-A-based polymers similar to FBE, as observed at temperatures between 65 and 80°C [8]. The slight decrease in permeability at higher temperatures is primarily caused by a decrease in the solubility of gas at elevated temperatures. As this study did not include gas sorption measurements, mathematical models for transport analysis could not be employed, because the presence of fugacity-based sorption parameters for CO_2 is a prerequisite for accurately fitting permeability data. However, literature data on glassy polymers suggest certain boundary limits for CO_2 dual sorption parameters, such as $10^{-6} < b_{CO_2} < 10^{-5}$ Pa^{-1} [31]. However, it is important to note that a fitting analysis based solely on the dual mode sorption model may not be a reliable predictor of permeability, especially when considering potential physical and chemical effects. For example, factors such as test temperature can have an impact on dual mode sorption parameters, which can lead to inaccuracies in predicting permeability.

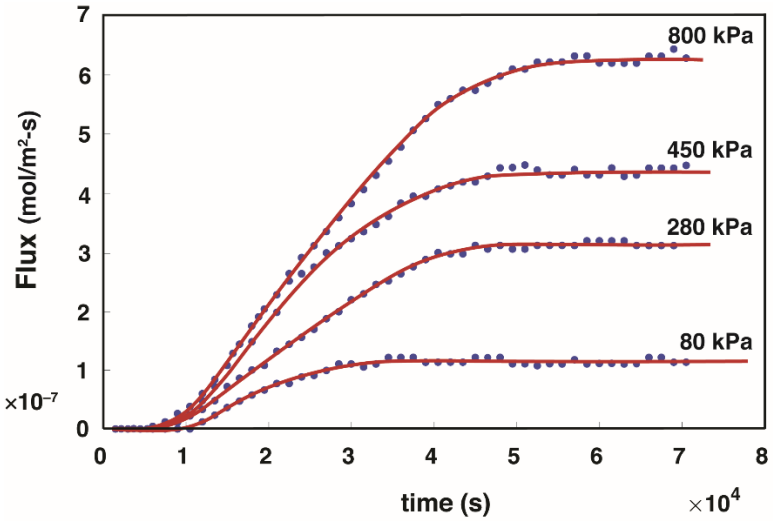

Fig. 3. Flux measurements at 65°C for FBE film with the upstream pressure of pure CO_2.

Table 1. Values of diffusion coefficient (m^2/s) of CO_2 in FBE determined from permeability measurements at dry-gas conditions.

Temperature (°C)	Thickness ± SD (μm)	Diffusion coefficient ± SD (m^2/s) × 10^{-13}
65	517 ± 41	5.3 ± 0.9
70	444 ± 62	6.7 ± 0.3
80	411 ± 49	9.1 ± 0.5

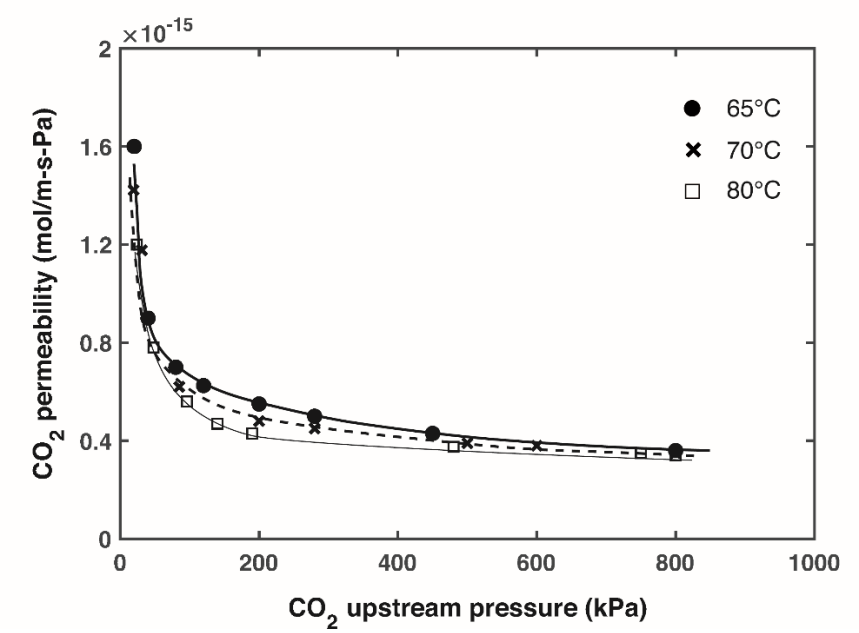

Fig. 4. CO_2 permeation isotherm in FBE in absence of water between 65 and 80°C. Lines are for guidance only.

The decrease in permeability with increasing pressure demonstrated that, similar to other glassy polymers such as polycarbonate, the CO_2 solubility coefficient of FBE is highly dependent on gas pressure [8]. This dependence resulted in a concave shape of the CO_2 permeability curve (Fig. 4). Also, since the mobility of CO_2 is generally an exponential function of concentration [8], CO_2 solubility increased more rapidly at lower pressures compared to higher pressures. Studies on glassy polymers [9], [32] have shown that the dependence of CO_2 permeability on upstream pressure generally follows the trend depicted schematically in Fig. 5. The lowest permeability at each temperature represents the plasticization pressure, at which the critical partial molar volume is attained and increased mobility in the typically tightly packed Henry's law region of the polymer structure is expected [33]. As external pipeline coatings are unlikely to be exposed to extremely high pressure environments and the plasticization pressure of glassy polymers caused by CO_2 gas is typically above 1 MPa [9], in this study, our investigation was confined to feed pressures lower than the minimum plasticization pressures for FBE. Indeed, applying higher pressures below the

plasticization threshold of 1 MPa can accelerate transport processes in epoxy coatings without changing degradation mechanisms. Higher CO_2 feed pressure, as per Eq. (8) and Fig. 4, primarily increases CO_2 flux throughout the coating, this in turn can aid in capturing under-coating reactions during shorter exposure experiments. To gain a comprehensive insight into the performance of the coating under this condition, we employed SEM/EDX analysis to study the impact of dry gas on the FBE microstructure. By analyzing selected areas of the SEM reference sample both before and after exposure to CO_2 at 800 kPa, as per Fig. 1, we were able to determine that the dry gas exposure had no adverse effect on the structural integrity of the FBE network or the filler component throughout the 120-hour exposure period.

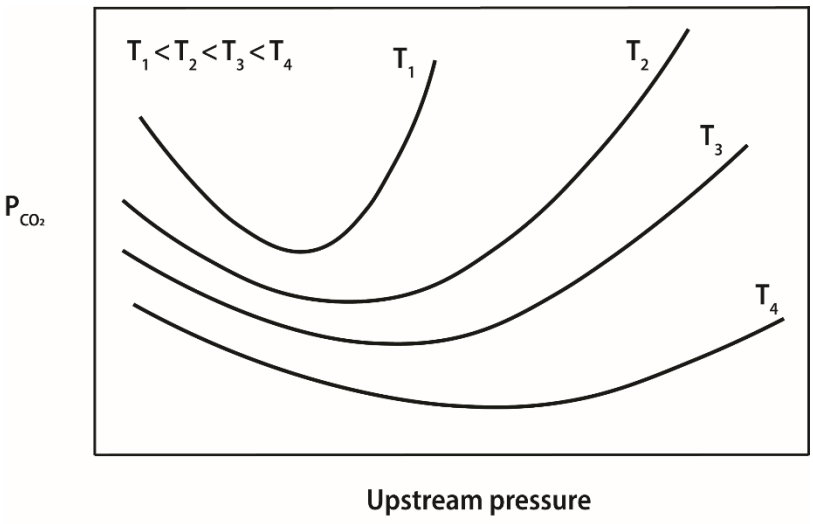

Fig. 5. Illustration of the typical effect of temperature on the permeability of glassy polymers against CO_2

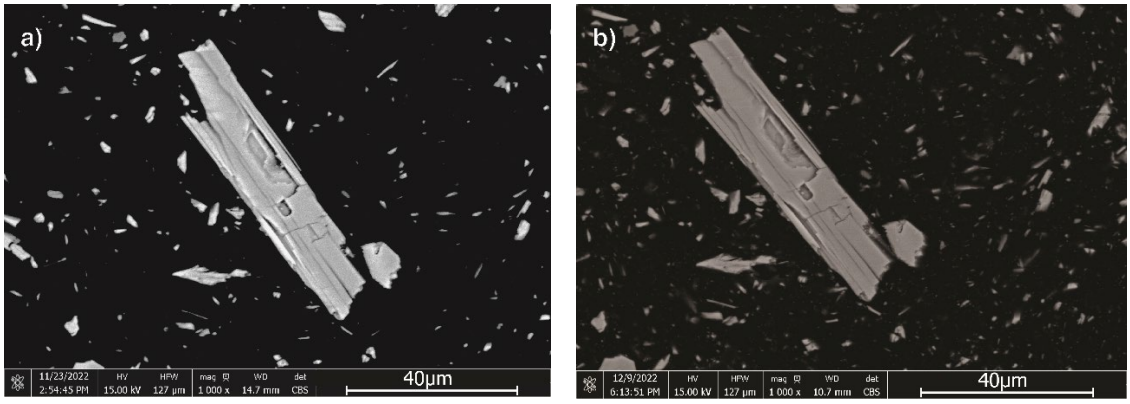

Fig. 6. Back-scattered electron image from FBE microstructure: a) before and b) after ~ 120 h exposure to dry CO_2 at 65°C and 800 kPa.

3.2. Wet-state permeation and degradation

The presence of water in the feed volume did not result in a significant competition between water and CO_2 for transport, contrary to what was observed with other gases such as oxygen [34]. Fig. 5 illustrates the slight increase in CO_2 permeability in wet conditions at 70°C, which is the median temperature (65 ≤T≤ 80°C). The permeability values in wet conditions at 65, 70, and 80°C were found to be similar, as shown by the solid line in Fig. 7. This is partly due to the comparable permeability at these temperatures in dry conditions (Fig. 4). At these test conditions, the epoxy coating only experienced plasticization effects from vapor pressure, not from CO_2 as the gas pressure range was lower than the critical p_{CO_2} (≪ 1 MPa). As a result, the polymeric network did not permit a significant gaseous flux. Additionally, it is noteworthy that small variations in steady-state flux (J_∞) were observed under wet-state conditions, as shown in in Fig. 8. These fluctuations made measurements more challenging compared to the dry gas system. This alternating pattern in flux values suggests a dynamic interplay between the two penetrants in terms of transport channels. By comparing the resulting microstructure after exposure to CO_2/H_2O with that of hydrothermally aged FBE [5], [16], we can discern the specific effects of each penetrant. As water permeates the FBE coating (at temperatures above 65°C), it causes degradation by plasticizing the epoxy network, leading to swelling and an increase in vapor transport [5]. Given that

microchannels within the coating greatly affect gas permeability, the segregation effects of the added CO_2 on the epoxy/coating are crucial to consider.

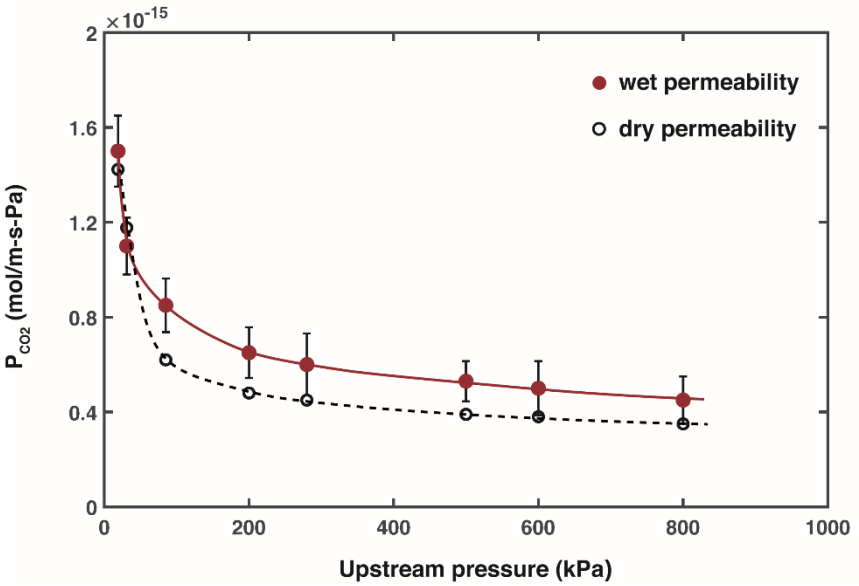

Fig. 7. Permeability of CO_2 at various upstream pressures in FBE for wet and dry conditions at 70°C. The vapor pressure under wet conditions was 31 kPa, equivalent to the saturation pressure of water vapor at 70°C.

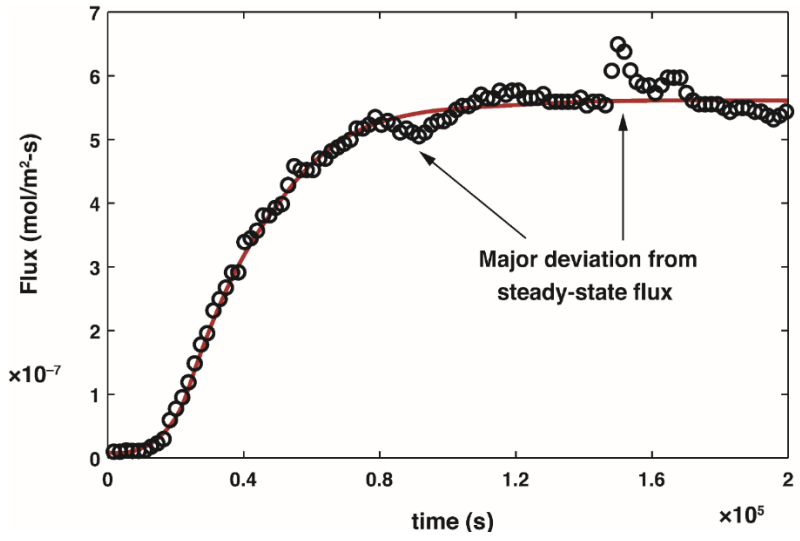

Fig. 8. CO_2 flux in downstream volume at 65°C and gas pressure of 800 kPa in the presence of water.

The surface of the SEM reference sample (exposed as per Fig. 1) revealed the transformation of filler particles as a result of exposure to a CO_2/H_2O environment (Fig. 8). The EDX analysis showed that the wollastonite fillers within the FBE matrix underwent carbonation transformation (from the surface towards the center) in this medium. The analysis showed that the surface of the filler after 120 hours of exposure to 800kPa CO_2 feed pressure at 65°C had significantly less calcium and more silicon, indicating the formation of silicon oxide on the filler surface as a result of the carbonation reaction [35]:

$$CaSiO_3 + CO_2 \xrightarrow{H_2O} CaCO_3 + SiO_2\ (amorphous) \quad (9)$$

Cross-sectional analysis of the sample membranes also showed higher concentrations of amorphous SiO_2 after permeation tests compared to an unexposed FBE sample. However, it should be noted that since the reaction is from the surface to the center of the wollastonite grains [36], cross-sectional analysis of film membranes might not provide reliable evidence for this characterization. The conversion of wollastonite into calcite ($CaCO_3$) and amorphous SiO_2 has been well-documented in literature concerning carbon capture and storage [35], [37]. Studies have shown that upon carbonation, the surface of wollastonite is covered with amorphous silica, rather than calcite, and the product layer may not be as porous as the amorphous silica layer formed in bulk solution [38]. This conversion of wollastonite into calcite and amorphous SiO_2 can open new microchannels for gas/vapor transport inside the coating network, which may have implications for the long-term performance of FBE coatings in CO_2-rich environments.

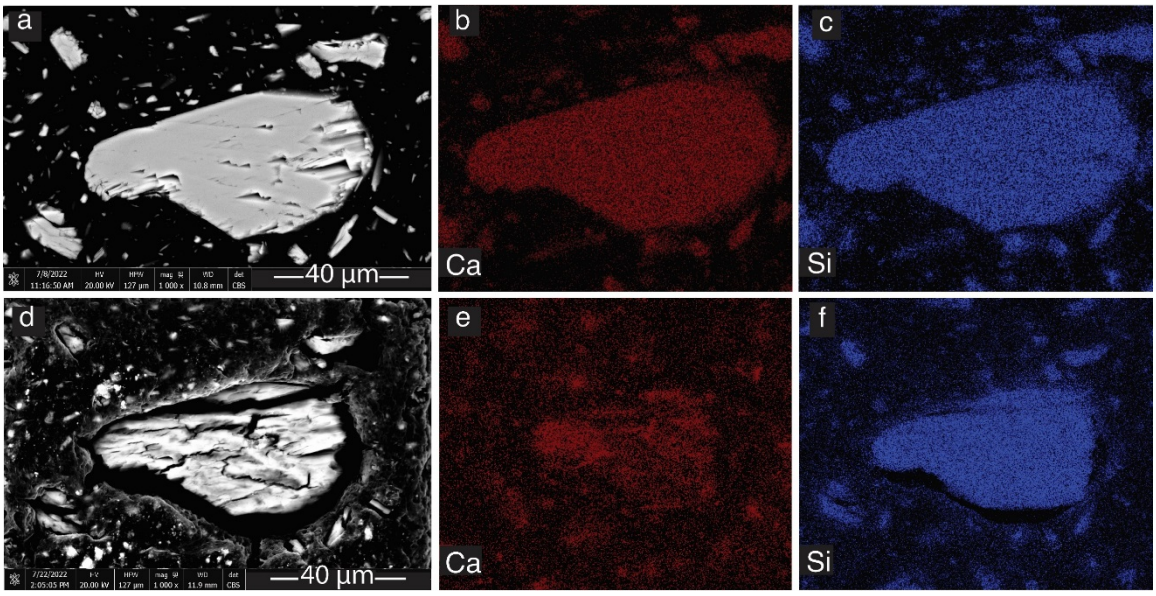

Fig. 8. Back-scattered electron image of a wollastonite filler (a) and its corresponding elemental mapping of calcium (b) and silicon (c) prior to and after (d-f) 120 h exposure to CO_2/H_2O mixture at 65°C.

We observed that the degradation of FBE coatings in a CO_2/H_2O atmosphere was not solely dependent on the temperature, as carbonation of wollastonite filler particles occurred even at temperatures lower than 65°C where water-induced plasticization was absent. Through SEM analysis (Fig. 9), we observed that the segregation of filler particles in CO_2/H_2O environments was distinct from degradation caused by water uptake, which only affects the epoxy network [5]. The carbonation of filler particles created microchannels and microcracks that greatly impacted gas transport in the coating. Initially, FBE demonstrated a significant resistance to CO_2 transport, with the gas flux remaining at zero for 48 hours (Fig. 10). However, prolonged exposure to CO_2/H_2O changed the barrier properties of the coating, developing diffusive channels for gas permeation even at room temperature conditions. Our investigations of permeability at ambient temperatures (25 and 40°C) revealed that, although the gas flux was insignificant for the first early stages (30 to 48 hours), gas passage through FBE was progressively facilitated, resulting in meaningful permeability values of 4×10^{-17} to 6×10^{-17} mol/m-s-Pa.

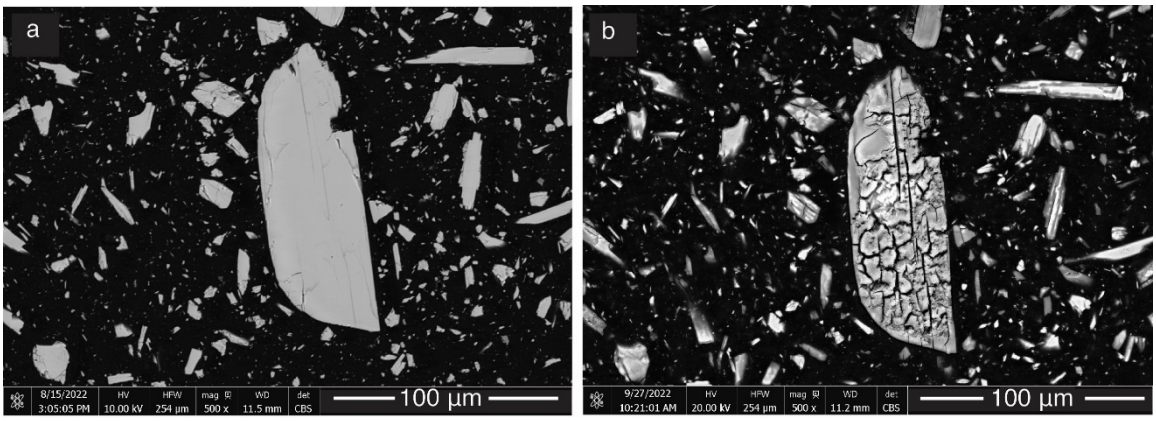

Fig. 9. Micrographs of a wollastonite filler inside the FBE network: a) before and b) after 120 h exposure to CO_2/H_2O mixture at 25°C.

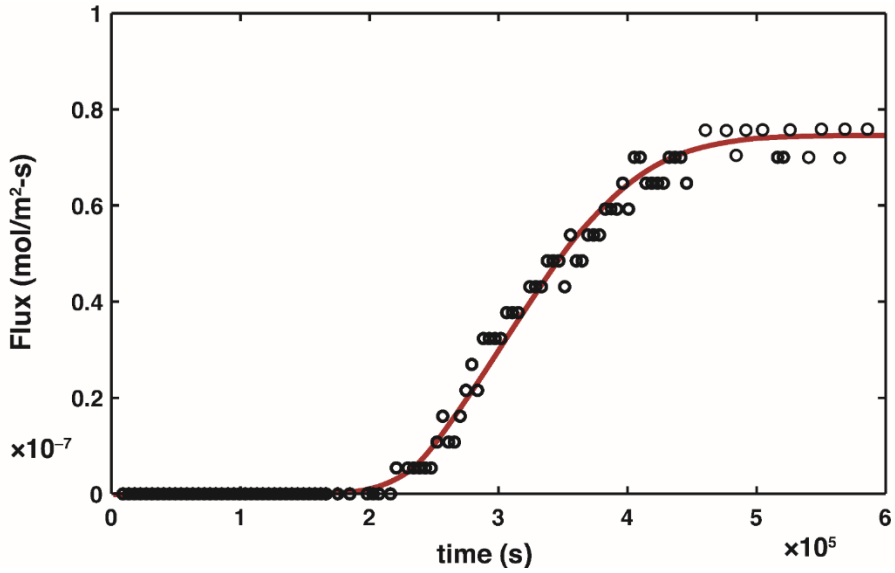

Fig. 10. CO_2 flux through FBE in the presence of water and upstream CO_2 pressure of 800 kPa at 25°C. The solid line was drawn between data points and is for guidance only.

3.3. Electrochemical performance evaluation of the FBE coated steel

EIS was used to evaluate the performance of a coating system on steel panels that had undergone prior exposure to hydrothermal conditions followed by exposure to a CO_2/H_2O environment.

Previous EIS characterizations of hydrothermally aged FBE-coated steel panels were used as a reference for this study and details can be found in [16]. The barrier properties of organic coating systems can rapidly change within a few minutes of immersion due to the percolation of electrolytes and the development of nano- or macro-structural defects over time [39]. The formation of pores in the outer layer (represented by R_{po} and CPE_{po}) and the high impedance of the preserved inner layer (represented by R_c and CPE_c) can be identified using an EEC to understand the system's behavior (Fig. 11). This representation is valid until a major coating failure, such as the formation of microcracks, takes place in the system [39]. In this model, R_s is the solution resistance and the constant phase elements (CPE) $(Y_0)_{dl}$ and $(Y_0)_c$ are used to represent the non-ideal capacitance behavior of the coating The impedance of the CPE is defined by the following equation [40], [41]:

$$Z_{CPE} = (Y_0)^{-1}(j\omega)^{-n} \quad (10)$$

where Y_0 has the units of $\Omega^{-1}cm^{-2}s^{(n-1)}$, j the imaginary number, n is the relaxation coefficient and its value ranges between zero and unity representing the deviation from purely capacitive behavior ($n = 1$, Y_0 behaves as an ideal capacitor), and ω is the angular frequency ($\omega = 2\pi f$, f is the frequency in Hz). Typically, an increase in coating capacitance occurs when water is transported through or adsorbed into the coating, which is caused by the high dielectric constant of the adsorbed water (78.3) in comparison to that of the polymeric coating (3-8) [42].

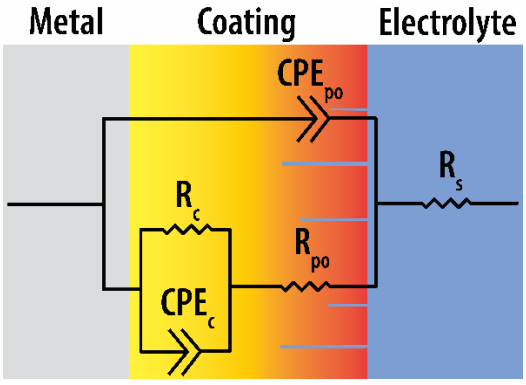

Fig. 11. EEC model used to simulate impedance spectra of the FBE-coated steel.

When the exposure duration to a CO_2/H_2O medium increases, certain changes occur that are linked to the carbonation of filler particles within the FBE matrix and the creation of micropores. These changes include the variation in the Z_{re} and a shift in phase angle, as shown in Fig. 12. Over the course of 310 hours, there was a marked decrease in R_c (from 3.12 x 10^{12} to 3 x 10^7 Ω), as demonstrated in Table 2. This decline is an indication of the extent of coating damage [39]. As time progressed, two significant changes were observed: a decrease in coating resistance and a shift in phase angle to negative values. These alterations are indicative of damage to the inner layers of the barrier coating, which allowed water to penetrate the coating. The coating's protective properties were thus compromised, rendering the underlying metal more susceptible to corrosion. The experimental and modelled impedance data are in excellent agreement as confirmed by the chi-squared values, which are less than 0.05. The coating's integrity during exposure to the CO_2/H_2O environment was assessed using R_c and R_{po} parameters. Initially, R_{po} increased, which was likely due to the plugging of the existing defects on the FBE surface as a result of carbonation of wollastonite fillers, as well as competitive transport of CO_2 and water through micropore channels. After 144 h of exposure, R_{po} decreased, which is likely due to the formation of micropores and cracks within the coating at the vicinity of filler particles. Additionally, the continuous decrease in R_c indicated that water was infiltrating the pores, and electrochemical reactions (e.g., oxidation of steel) were progressing more readily at the coating/substrate interface. The SEM images of the reference sample in Fig. 8 confirmed that carbonation of fillers within the FBE microstructure can damage the coating. Compared to earlier investigations on ageing in water alone [16], the changes in the coating impedance were significantly greater over this short exposure period, highlighting the adverse effects of the aggressive CO_2/H_2O atmosphere on the FBE's barrier properties.

Table 2. Quantitative information on the impedance spectra of the FBE-coated steel was obtained by simulating the EEC and fitting it to the experimental spectra. Parameters indicate the performance of the coating and progress of electrochemical processes at the coating/substrate

interface after up to 310 hours of exposure to humidified CO_2 at 65°C (p_{CO_2} = 800 kPa). All measurements were carried out on a 9.27 cm^2 test area of the coated steel panel.

Time	$(Y_0)_{po} \times 10^{10}$	n_{po}	$R_{po} \times 10^{-10}$	$(Y_0)_c \times 10^7$	n_c	$R_c \times 10^{-10}$	Chi-squared
h	$s^n\Omega^{-1}$	–	Ω	$s^n\Omega^{-1}$	–	Ω	–
0	1.910	0.953	8.86	0.121	0.250	312	0.0388
70	1.340	0.982	6.75	4.540	0.005	5.736	0.0129
144	1.221	0.932	57.6	226.60	0.028	0.009	0.0020
220	1.341	0.928	14.5	8.03	0.170	0.004	0.0377
310	1.407	0.973	13.50	146.70	0.975	0.003	0.0102

a)

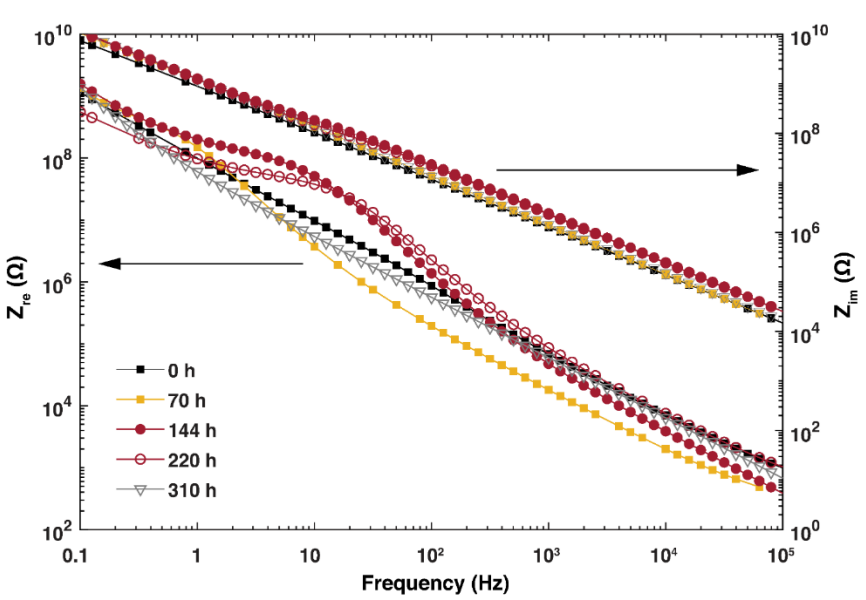

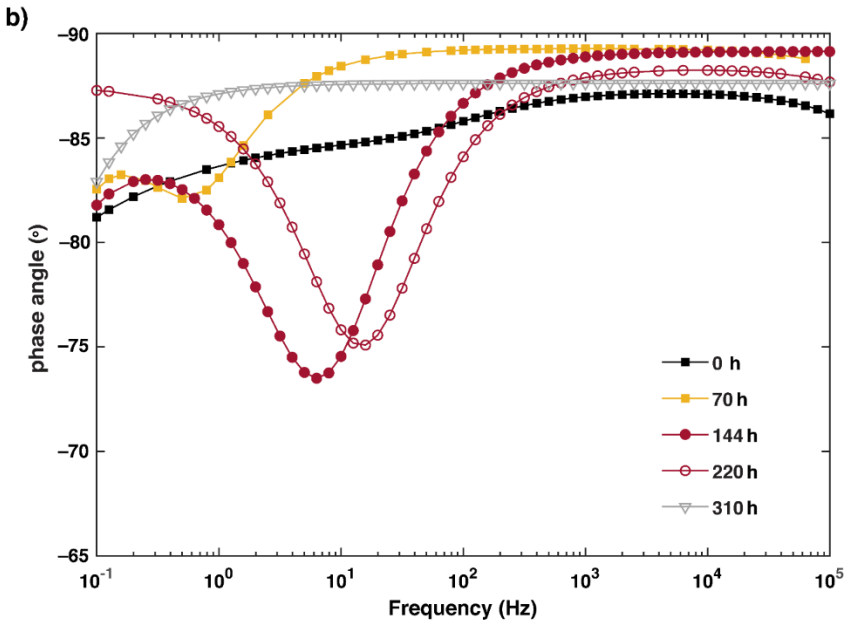

Fig. 12. Impedance spectra: a) Bode impedance and b) Bode phase angle plots of the FBE-coated steel panels exposed to humidified CO_2 at 65°C and p_{CO_2} = 800 kPa as a function of ageing times.

The accelerated exposure tests in this study were more severe than those experienced by real-life conditions for pipes. Thus, degradation and micro-channel formation caused by carbonation may take longer to manifest in real-life scenarios. We should note that when wollastonite fillers are exposed to water under ambient pressures and 60°C, carbonation reactions occur rapidly (within 10 to 24 hours) [43], resulting in anticipated degradation from CO_2/H_2O media within the first 100 days of service [16]. Using the measured permeability data, the critical p_{CO_2} for underlying corrosion can be calculated based on an average corrosion rate of < 0.05 mm/y for a 20-year pipeline service life [44]. For a 400 µm average coating thickness, the maximum p_{CO_2} that yields a gas flux within the corrosion allowance would be ~ 90 kPa under conditions of local saturation of CO_2. This finding indicates that even under high concentrations of CO_2 that can occur locally, severe damage to the under-coating steel pipe could occur over the long term. Our experiment suggests that exposure to CO_2/H_2O media can affect coating performance even with adhesion forces, resulting in micro-channel formation that could affect species transport, especially at high temperatures [34].

4. Conclusion

CO_2-rich atmospheres in combination with moisture can be highly detrimental to FBE-coated pipelines. This is due not only to the high transport rate of CO_2 within the polymeric network, but also to degradation effects caused by the carbonation of filler components within the FBE. Our measurements showed that CO_2 has a relatively high permeability in dry diffusion systems, about one order of magnitude higher than that of oxygen. Contrary to the expected tradeoff relationship between gas pair permeabilities, the permeability of CO_2 shows a slight increase in wet environments. Our observations of fluctuations in gas/vapor flux provide evidence of dynamic changes occurring within the coating membrane. Microstructural examinations confirmed that wollastonite filler particles in FBE experience a carbonation reaction, resulting in the formation of microchannels on the interface between fillers and the epoxy network. Electrochemical impedance analysis showed a continuous decrease in the resistance of the FBE coating when exposed to a CO_2/H_2O mixture. Furthermore, changes in the pore resistance of the coating were observed, which were attributed to the carbonation of filler particles on the surface and within the coating. The minimum of the phase angle in the capacitive-resistive transition region moved to higher frequencies which signal the degradation of the barrier coating. It is important to note that these effects can occur at ambient temperatures (i.e., 25 and 40°C) and pressures (< 100 kPa). High concentrations of CO_2 and H_2O near FBE can cause severe degradation of the epoxy network and filler particles in the coating, leading to carbonation and swelling, respectively. As a result, the coating's barrier properties are compromised, allowing for increased gas permeation and weakening its ability to protect the steel structure from corrosion.

Acknowledgment

The authors acknowledge funding support from the Natural Sciences and Engineering Research Council (NSERC) of Canada [NSERC CRDPJ 503725-16]. The funding and in-kind support from

Shawcor Ltd. and Specialty Polymer Coatings Inc. [Industry portion - NSERC CRDPJ 503725-16] are also greatly appreciated.

References

[1] N. Rajagopalan, C. E. Weinell, K. Dam-Johansen, and S. Kiil, “Influence of CO2at HPHT Conditions on the Properties and Failures of an Amine-Cured Epoxy Novolac Coating,” *Ind. Eng. Chem. Res.*, vol. 60, no. 41, pp. 14768–14778, 2021, doi: 10.1021/acs.iecr.1c02713.

[2] K. Majchrowicz, T. Brynk, M. Wieczorek, D. Miedzińska, and Z. Pakieła, “Exploring the susceptibility of P110 pipeline steel to stress corrosion cracking in CO2-rich environments,” *Eng. Fail. Anal.*, vol. 104, no. June, pp. 471–479, 2019, doi: 10.1016/j.engfailanal.2019.06.016.

[3] M. Dai, “In situ mathematically simulation for CO2 internal corrosion in wet natural gas gathering pipelines system by HYSYS,” *Eng. Fail. Anal.*, vol. 122, no. February, p. 105265, 2021, doi: 10.1016/j.engfailanal.2021.105265.

[4] Y. Xiang, C. Li, W. Hesitao, Z. Long, and W. Yan, “Understanding the pitting corrosion mechanism of pipeline steel in an impure supercritical CO2 environment,” *J. Supercrit. Fluids*, vol. 138, no. April, pp. 132–142, 2018, doi: 10.1016/j.supflu.2018.04.009.

[5] H. Zargarnezhad, E. Asselin, D. Wong, and C. N. C. Lam, “Water transport through epoxy-based powder pipeline coatings,” *Prog. Org. Coatings*, vol. 168, no. March, p. 106874, 2022, doi: 10.1016/j.porgcoat.2022.106874.

[6] C. A. Scholes, S. Kanehashi, G. W. Stevens, and S. E. Kentish, “Water permeability and competitive permeation with CO2 and CH4 in perfluorinated polymeric membranes,” *Sep. Purif. Technol.*, vol. 147, pp. 203–209, 2015, doi: 10.1016/j.seppur.2015.04.023.

[7] C. A. Scholes, J. Jin, G. W. Stevens, and S. E. Kentish, “Competitive permeation of gas and water vapour in high free volume polymeric membranes,” *J. Polym. Sci. Part B*

Polym. Phys., vol. 53, no. 10, pp. 719–728, 2015, doi: 10.1002/polb.23689.

[8] M. Minelli and G. C. Sarti, “Permeability and diffusivity of CO2 in glassy polymers with and without plasticization,” *J. Memb. Sci.*, vol. 435, pp. 176–185, 2013, doi: 10.1016/j.memsci.2013.02.013.

[9] A. Bos, I. G. M. Punt, M. Wessling, and H. Strathmann, “CO2 -induced plasticization phenomena in glassy polymers,” *J. Memb. Sci.*, vol. 155, pp. 67–78, 1999.

[10] L. Ansaloni, B. Alcock, and T. A. Peters, “Effects of CO2 on polymeric materials in the CO2 transport chain: A review,” *Int. J. Greenh. Gas Control*, vol. 94, no. August 2019, p. 102930, 2020, doi: 10.1016/j.ijggc.2019.102930.

[11] M. Watanabe, Y. Hashimoto, T. Kimura, and A. Kishida, “Characterization of engineering plastics plasticized using supercritical CO2,” *Polymers (Basel).*, vol. 12, no. 1, 2020, doi: 10.3390/polym12010134.

[12] C. J. Anderson, W. Tao, C. A. Scholes, G. W. Stevens, and S. E. Kentish, “The performance of carbon membranes in the presence of condensable and non-condensable impurities,” *J. Memb. Sci.*, vol. 378, no. 1–2, pp. 117–127, 2011, doi: 10.1016/j.memsci.2011.04.058.

[13] G. M. Geise, D. R. Paul, and B. D. Freeman, “Fundamental water and salt transport properties of polymeric materials,” *Prog. Polym. Sci.*, vol. 39, no. 1, pp. 1–24, 2014, doi: 10.1016/j.progpolymsci.2013.07.001.

[14] R. A. De Motte, R. Barker, D. Burkle, S. M. Vargas, and A. Neville, “The early stages of FeCO3 scale formation kinetics in CO2 corrosion,” *Mater. Chem. Phys.*, vol. 216, pp. 102–111, 2018, doi: https://doi.org/10.1016/j.matchemphys.2018.04.077.

[15] E. Bardal, *Corrosion and protection against corrosion. – (Engineering materials and processes)*, no. 148, Jan.1979. 2004.

[16] H. Zargarnezhad, E. Asselin, D. Wong, and C. N. C. Lam, “Quantitative performance assessment of epoxy-based pipeline coatings: Hydrothermal exposure,” *Corros. Sci.*, 2023.

[17] T. Tanupabrungsun, B. Brown, and S. Nesic, “Effect of pH on CO2 corrosion of mild steel at elevated temperatures,” *NACE - Int. Corros. Conf. Ser.*, no. 2348, pp. 1–11, 2013.

[18] T. Tanupabrungsun, “Thermodynamics and Kinetics of Carbon Dioxide Corrosion of Mild Steel at Elevated Temperatures,” the Russ College of Engineering and Technology of Ohio University, 2013.

[19] B. Beverskog, “Revised Diagrams for Iron At 25-300 ° C,” *Science (80-.).*, vol. 38, no. 12, pp. 2121–2135, 1996, [Online]. Available: http://www.sciencedirect.com/science/article/pii/S0010938X96000674.

[20] M. Xu, C. N. C. Lam, D. Wong, and E. Asselin, “Evaluation of the cathodic disbondment resistance of pipeline coatings – A review,” *Prog. Org. Coatings*, vol. 146, p. 105728, 2020, doi: 10.1016/j.porgcoat.2020.105728.

[21] Z. Shao *et al.*, “High-pressure induced acceleration pathways for water diffusion in heavy duty anticorrosion coatings under deep ocean environment: (I) The samples subjected to high-pressure pre-processing,” *Prog. Org. Coatings*, vol. 170, no. March, p. 106948, 2022, doi: 10.1016/j.porgcoat.2022.106948.

[22] A. J. Kandeloos and M. M. Attar, “The diffusion and adhesion relationship between free films and epoxy coated mild steel,” *Prog. Org. Coatings*, no. September, 2019, doi: 10.1016/j.porgcoat.2019.105405.

[23] P. A. Saliba, A. A. Mansur, D. B. Santos, and H. S. Mansur, “Fusion-bonded epoxy composite coatings on chemically functionalized API steel surfaces for potential deep-water petroleum exploration,” *Appl. Adhes. Sci.*, vol. 3, no. 1, 2015, doi: 10.1186/s40563-015-0052-2.

[24] P. A. Saliba, A. A. P. Mansur, and H. S. Mansur, “Advanced Nanocomposite Coatings of Fusion Bonded Epoxy Reinforced with Amino-Functionalized Nanoparticles for Applications in Underwater Oil Pipelines,” *J. Nanomater.*, vol. 2016, 2016, doi: 10.1155/2016/7281726.

[25] E. Legghe, E. Aragon, L. Bélec, A. Margaillan, and D. Melot, “Correlation between water

diffusion and adhesion loss: Study of an epoxy primer on steel," *Prog. Org. Coatings*, vol. 66, no. 3, pp. 276–280, 2009, doi: 10.1016/j.porgcoat.2009.08.001.

[26] ASTM, *Standard Test Method for Nondestructive Measurement of Dry Film Thickness of Applied Organic Coatings Using an Ultrasonic Gage (ASTM D 6132)*, no. Reapproved 2017. West Conshohocken, 2017, pp. 8–10.

[27] T. C. Merkel, V. Bondar, K. Nagai, and B. D. Freeman, "Hydrocarbon and perfluorocarbon gas sorption in poly(dimethylsiloxane), poly(1-trimethylsilyl-1-propyne), and copolymers of tetrafluoroethylene and 2,2-bis(trifluoromethyl)-4,5-difluoro-1,3-dioxole," *Macromolecules*, vol. 32, no. 2, pp. 370–374, 1999, doi: 10.1021/ma9814402.

[28] M. C. Celina and A. Quintana, "Oxygen diffusivity and permeation through polymers at elevated temperature," *Polymer (Guildf).*, vol. 150, pp. 326–342, 2018, doi: 10.1016/j.polymer.2018.06.047.

[29] U. Sonchaeng, F. Iñiguez-Franco, R. Auras, S. Selke, M. Rubino, and L. T. Lim, "Poly(lactic acid) mass transfer properties," *Prog. Polym. Sci.*, vol. 86, pp. 85–121, 2018, doi: 10.1016/j.progpolymsci.2018.06.008.

[30] H. Zargarnezhad, E. Asselin, D. Wong, and C. Lam, "A critical review of the time-dependent performance of polymeric pipeline coatings: Focus on hydration of epoxy-based coatings," *Polymers (Basel).*, vol. 13, no. 9, p. 1517, 2021, doi: 10.3390/polym13091517.

[31] C. A. Scholes, S. E. Kentish, and G. W. Stevens, "Effects of minor components in carbon dioxide capture using polymeric gas separation membranes," *Sep. Purif. Rev.*, vol. 38, no. 1, pp. 1–44, 2009, doi: 10.1080/15422110802411442.

[32] K. Okamoto, K. Tanaka, T. Shigematsu, H. Kita, A. Nakamura, and Y. Kusuki, "Sorption and transport of carbon dioxide in a polyimide from 3,3′,4,4′-biphenyltetracarboxylic dianhydride and dimethyl-3,7-diaminodibenzothiophene-5,5-dioxide," *Polymer (Guildf).*, vol. 31, pp. 673–678, 1990.

[33] X. Duthie, S. Kentish, C. Powell, K. Nagai, G. Qiao, and G. Stevens, "Operating

temperature effects on the plasticization of polyimide gas separation membranes," *J. Memb. Sci.*, vol. 294, no. 1–2, pp. 40–49, 2007, doi: 10.1016/j.memsci.2007.02.004.

[34] H. Zargarnezhad, P. Zarei, D. Wong, C. N. C. Lam, and E. Asselin, "Oxygen transport through epoxy-based powder coatings in humid environments," *Prog. Org. Coatings*, vol. 175, no. July 2022, p. 107295, 2022, doi: 10.1016/j.porgcoat.2022.107295.

[35] K. Svensson, A. Neumann, F. Feitosa Menezes, C. Lempp, and H. Pöllmann, "Carbonation of natural pure and impure wollastonite," *SN Appl. Sci.*, vol. 1, no. 4, pp. 1–12, 2019, doi: 10.1007/s42452-019-0328-4.

[36] K. Svensson, A. Neumann, F. F. Menezes, C. Lempp, and H. Pöllmann, "The conversion of wollastonite to CaCO3 considering its use for CCS application as cementitious material," *Appl. Sci.*, vol. 8, no. 2, pp. 1–18, 2018, doi: 10.3390/app8020304.

[37] F. Di Lorenzo *et al.*, "The carbonation of wollastonite: A model reaction to test natural and biomimetic catalysts for enhanced CO2 sequestration," *Minerals*, vol. 8, no. 5, 2018, doi: 10.3390/min8050209.

[38] Y. Min, Q. Li, M. Voltolini, T. Kneafsey, and Y. S. Jun, "Wollastonite Carbonation in Water-Bearing Supercritical CO2: Effects of Particle Size," *Environ. Sci. Technol.*, vol. 51, no. 21, pp. 13044–13053, 2017, doi: 10.1021/acs.est.7b04475.

[39] A. Trentin, A. Pakseresht, A. Duran, Y. Castro, and D. Galusek, "Electrochemical Characterization of Polymeric Coatings for Corrosion Protection: A Review of Advances and Perspectives," *Polymers (Basel).*, vol. 14, no. 12, p. 2306, 2022, doi: 10.3390/polym14122306.

[40] C. Fan, J. Shi, and K. Dilger, "Water uptake and interfacial delamination of an epoxy-coated galvanized steel: An electrochemical impedance spectroscopic study," *Prog. Org. Coatings*, vol. 137, no. August, p. 105333, 2019, doi: 10.1016/j.porgcoat.2019.105333.

[41] F. Mahdavi, M. Y. J. Tan, and M. Forsyth, "Electrochemical impedance spectroscopy as a tool to measure cathodic disbondment on coated steel surfaces: Capabilities and limitations," *Prog. Org. Coatings*, vol. 88, pp. 23–31, 2015, doi:

10.1016/j.porgcoat.2015.06.010.

[42] A. S. Castela and A. M. Simões, “Assessment of water uptake in coil coatings by capacitance measurements,” *Prog. Org. Coatings*, vol. 46, no. 1, pp. 55–61, 2003, doi: 10.1016/S0300-9440(02)00190-X.

[43] E. Gartner and H. Hirao, “A review of alternative approaches to the reduction of CO2 emissions associated with the manufacture of the binder phase in concrete,” *Cem. Concr. Res.*, vol. 78, pp. 126–142, 2015, doi: 10.1016/j.cemconres.2015.04.012.

[44] A. Bahadori, “Corrosion in Pipelines and Piping Systems,” in *Oil and Gas Pipelines and Piping Systems*, Elsevier Inc., 2017, pp. 395–481.